Amplitude death in globally coupled oscillators with time-scale diversity

Wei Zou,[1,*] Meng Zhan,[2] and Jürgen Kurths[3,4,5]

[1]*School of Mathematical Sciences, South China Normal University, Guangzhou 510631, People's Republic of China*

[2]*State Key Laboratory of Advanced Electromagnetic Engineering and Technology, School of Electrical and Electronic Engineering, Huazhong University of Science and Technology, Wuhan 430074, China*

[3]*Potsdam Institute for Climate Impact Research, Telegraphenberg, Potsdam D-14415, Germany*

[4]*Institute of Physics, Humboldt University Berlin, Berlin D-12489, Germany*

[5]*Saratov State University, 4410012 Saratov, Russia*

(Received 10 September 2018; revised manuscript received 9 November 2018; published 12 December 2018)

We analyze amplitude death (AD) in large systems of globally coupled oscillators with randomly distributed time scales. We show that the distribution of characteristic eigenvalues of a large but finite system is well approximated by the continuous and discrete spectra of the system in the thermodynamic limit. The stability analysis from the continuous and discrete spectra of the infinite system provides a fairly accurate prediction for the onset of AD in the large finite system. We prove the argument by examining the stability of AD in a paradigmatic system of coupled Stuart-Landau limit cycles with mismatched time scales. The proposed technique is extended to systems of globally coupled nonlinear oscillators of a general form with time-scale diversity, which is verified in coupled chaotic Rössler oscillators. Our study provides analytical insight into the understanding of the emergence of AD in populations of globally coupled dynamical systems.

DOI: 10.1103/PhysRevE.98.062209

I. INTRODUCTION

The collective behaviors of large numbers of coupled nonlinear oscillators have attracted a great deal of interest among researchers in diverse branches of science and technology [1–3]. This interest is due to the fact that an ensemble of coupled nonlinear oscillators provides a simple but efficient mathematical model to both qualitatively and quantitatively describe dynamical activities emerging in nature and engineering. One such intriguing behavior is amplitude death (AD), which refers to quenching of oscillations due to coupling-induced stabilization of an unstable homogeneous steady state [4,5]. From the control point of view, AD can be regarded as a stabilization of an unstable behavior in coupled systems, which is deemed relevant for potential applications in practical systems, such as in the stabilization of a particular fixed-point state of coupled lasers [6] and the suppression of high-amplitude pressure oscillations in thermoacoustic engines [7,8]. The phenomenon of AD in coupled oscillators has been studied for almost three decades [9,10]. Initially, AD was observed in coupled oscillators with a large mismatch of parameters [9]. Later on, AD was further reported in coupled identical oscillators with diverse coupling schemes, such as time-delayed coupling [11–16], dynamical coupling [17–19], conjugate coupling [20–22], indirect coupling [23–25], mean-field diffusion [26–29], etc.

In many natural systems, parameter mismatch is inevitable and prevalent, and it is introduced by a distribution of intrinsic frequencies or a heterogeneity of subunits. Thus, it is of practical importance to unravel the underlying mechanisms of AD and its behavior in systems of coupled nonidentical oscillators. Since the discovery of AD by Yamaguchi and Shimizu in 1984 [9], it has been exploited extensively in different circumstances [4]. In particular, a number of efforts have been devoted to the emergence of AD in coupled Stuart-Landau limit-cycle oscillators with mismatched natural frequencies. The occurrence of AD in coupled Stuart-Landau oscillators is indicated by the observation that the oscillators pull each other off their stable limit cycles and collapse to the unstable origin. Hitherto, significant theoretical progress have been achieved for two or more populations of Stuart-Landau oscillators with global coupling. For example, Aronson *et al.* [30] derived the exact conditions for the onset of AD in two coupled Stuart-Landau oscillators with disparate frequencies. Ermentrout [31] calculated the stability boundaries of AD of globally coupled Stuart-Landau oscillators for several specific frequency distributions. Mirollo and Strogatz [32] further analyzed the rigorous stability of AD in a large number of globally coupled Stuart-Landau oscillators with randomly distributed frequencies. On the other hand, extensive numerical studies of AD have been done for nonidentical Stuart-Landau oscillators on regular one-dimensional arrays [33–36] and complex topological networks [37–39].

The model of coupled Stuart-Landau limit-cycle oscillators serves as a paradigmatic and ideal framework for exploring AD, where the intrinsic frequency is a parameter directly characterizing the speed of the periodic motion of each uncoupled element. By introducing time scales in coupled oscillators of a general form, Monte *et al.* [40] showed that AD is a ubiquitous phenomenon even in coupled chaotic oscillators in the presence of large time-scale dispersion and strong coupling, which can be regarded as a generalization of AD in Stuart-Landau limit-cycle oscillators with different natural

*weizou83@gmail.com

frequencies. Monte *et al.* proposed a novel technique of *order-parameter expansion* [41] to reduce the mean-field dynamics of globally coupled systems to a system of two coupled macroscopic variables, where they found that the onset of AD in the reduced low-dimensional system is an approximate prediction of AD in the original mean-field system [40]. However, Monte *et al.* [40] did not provide information about the stability property of AD in the original full mean-field system.

In this work, via a rigorous stability analysis, we study the emergence of AD in systems of globally coupled nonlinear oscillators with dispersed time scales. We determine the stability of AD from the distribution of characteristic eigenvalues of a full coupled system, rather than from a reduced system such as the method of *order-parameter expansion* in Ref. [40]. We find that the distribution of eigenvalues can be nicely predicted by the continuous and discrete spectra of the system in its thermodynamic limit. Thus we argue that the onset conditions of AD in a large system are in fairly good agreement with those of the system with an infinite number of elements. The infinite system provides an accurate description of AD in a large but finite system of globally coupled oscillators with distributed time scales. We elaborate on the argument by performing a detailed study of AD in globally coupled Stuart-Landau oscillators with uniformly distributed time scales. We further extend our results to globally coupled oscillators of a general form with different time scales, which is well exemplified in coupled chaotic Rössler oscillators. Our scheme is elementary and rigorous, thus it leads to a better prediction of AD in coupled systems with time-scale diversity.

II. RESULTS AND OBSERVATIONS

A. Coupled Stuart-Landau oscillators

Let us start to consider a global population of diffusively coupled Stuart-Landau oscillators with disparate time scales defined by the equation

$$\dot{Z}_j = \tau_j(1 + i w_j - |Z_j|^2)Z_j + \frac{K}{N}\sum_{k=1}^{N}(Z_k - Z_j), \quad (1)$$

where $Z_j(t)$ $(j = 1, \ldots, N)$ is a complex variable that denotes the dynamic state of the jth oscillator at time t, w_j is the intrinsic frequency of each uncoupled oscillator, and $K \geqslant 0$ is the coupling strength. The τ_j is a strictly positive number, which rescales the speed along the original orbit of an uncoupled oscillator. The time scales τ_j's are sampled within $[1-\sigma, 1+\sigma]$ according to a prescribed distribution $g(\tau)$. The above system (1) may be regarded as a generalization of coupled Stuart-Landau oscillators with different intrinsic frequencies, where AD in Stuart-Landau oscillators with dispersed frequencies has been extensively explored in the literature [30–39].

In the absence of coupling $K = 0$, each oscillator has an asymptotically stable limit-cycle motion $Z_j(t) = e^{i w_j \tau_j t}$ and an unstable equilibrium point at $Z_j = 0$. In the presence of coupling strength $K > 0$, the static solution $Z_j = 0$ always exists for the coupled system, which is the state of AD. Depending on the value of K and the distribution of τ_j, the AD state may be stabilized. In the following, we will identify the precise conditions under which the coupled system (1) experiences AD by performing a standard linear stability analysis.

The linearization of the coupled system (1) at $Z_j = 0$ is

$$\dot{z}_j = \left[\tau_j(1 + i w_j) - \left(1 - \frac{1}{N}\right)K\right]z_j + \frac{K}{N}\sum_{k=1,\,k\neq j}^{N} z_k. \quad (2)$$

For AD to be stable, all characteristic eigenvalues λ_j of the above linearized system are needed to satisfy $\mathrm{Re}(\lambda_j) < 0$. Let A be the characteristic matrix of (2), whose elements are given by

$$A_{jk} = \begin{cases} \frac{K}{N} & \text{if } j \neq k, \\ \tau_j(1 + i w_j) - \left(1 - \frac{1}{N}\right)K & \text{if } j = k. \end{cases} \quad (3)$$

Its eigenvalues λ_j are obtained by solving $|A - \lambda I_N| = 0$ (with I_N denoting the N-dimensional identity matrix), i.e.,

$$\begin{vmatrix} l_1 - \lambda & \frac{K}{N} & \cdots & \frac{K}{N} \\ \frac{K}{N} & l_2 - \lambda & \cdots & \frac{K}{N} \\ \vdots & \vdots & \ddots & \vdots \\ \frac{K}{N} & \frac{K}{N} & \cdots & l_N - \lambda \end{vmatrix} = 0, \quad (4)$$

where $l_j = \tau_j(1 + i w_j) - (1 - 1/N)K$. By factoring out a term $\tau_j(1 + i w_j) - K - \lambda$ from each jth row, the expression for Eq. (4) can be compactly written as a product of two factors,

$$\prod_{j=1}^{N}[\tau_j(1 + i w_j) - K - \lambda] \times \left[1 + \frac{K}{N}\sum_{j=1}^{N}\frac{1}{\tau_j(1 + i w_j) - K - \lambda}\right] = 0, \quad (5)$$

where the first factor represents the continuous spectrum, and the second one gives the discrete spectrum.

Without any diversity in both the time scales and the intrinsic frequencies, i.e., $\tau_j = 1$ and $w_j = w$ for all $j = 1, \ldots, N$, it is easy to see that $\lambda = 1 + i w$ is a solution for the discrete spectrum, i.e., AD is impossible for any values of K. For $\sigma > 0$, in general, the discrete spectrum λ in Eq. (5) cannot be analytically derived, as they rely on the specific samples of both τ_j and w_j $(j = 1, \ldots, N)$. However, the problem gets considerably simplified and can be analytically tractable in the thermodynamic limit $N \to \infty$ for identical frequencies $w_j = w$. In the case of $N \to \infty$ and $w_j = w$, the equation for the discrete spectrum can be replaced by an integral written as

$$\frac{1}{K} = \int_{1-\sigma}^{1+\sigma}\frac{g(\tau)d\tau}{\lambda + K - \tau(1 + i w)}. \quad (6)$$

Generally, the discrete spectrum λ in Eq. (6) cannot be derived explicitly. However, for a uniform distribution

$$g(\tau) = \begin{cases} \frac{1}{2\sigma}, & |\tau - 1| \leqslant \sigma, \\ 0, & |\tau - 1| > \sigma, \end{cases} \quad (7)$$

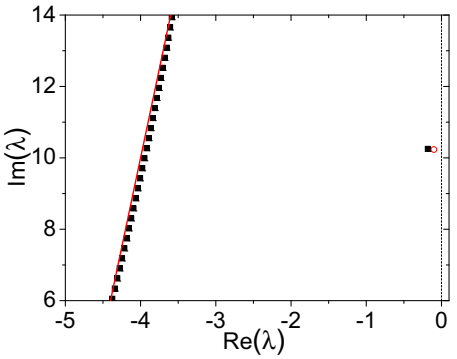

FIG. 1. Distribution of eigenvalues of the coupled system (2) with $N = 30$, $K = 5$, $w_j = 10$, and $\sigma = 0.4$. The time scales τ_j's are uniformly distributed on $[1-\sigma, 1+\sigma]$. The black squares denote the eigenvalues numerically obtained from the characteristic equation (4), which can be nicely predicted by the discrete and continuous spectra in Eqs. (8) and (9) represented by the red open circle and the red line, respectively. All eigenvalues have a negative real part implying that AD is stable.

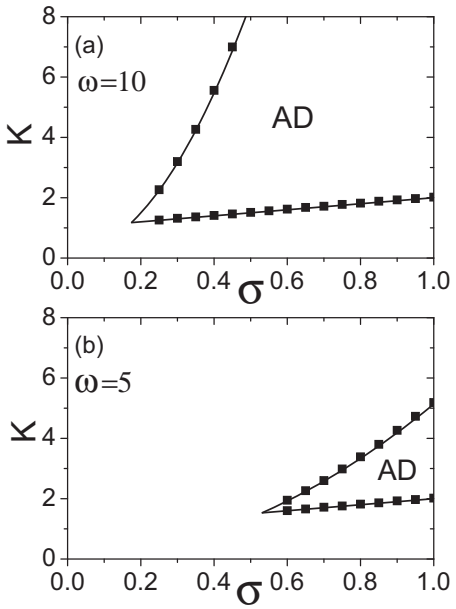

FIG. 2. Stability regions for AD of the coupled system (1) with $N = 30$ in the parameter space of (σ, K) for (a) $w = 10$ and (b) $w = 5$. The black squares are numerical results for the AD boundary obtained from directly integrating the coupled system (1), where the lower and upper black lines are the theoretical predictions by Eqs. (10) and (11), respectively. The time scales τ_j's are sampled from a uniform distribution over $[1-\sigma, 1+\sigma]$.

the expression of the discrete spectrum λ can now be worked out as

$$\lambda_{\mathrm{DS}} = \frac{2\sigma(1+iw)}{\exp\left[\frac{2\sigma(1+iw)}{K}\right]-1} - K + (1+\sigma)(1+iw). \quad (8)$$

On the other hand, the continuous spectrum comes directly from the first factor of Eq. (5) given by

$$\lambda_{\mathrm{CS}} = \tau(1+iw) - K, \quad \text{where} \quad 1-\sigma \leqslant \tau \leqslant 1+\sigma, \quad (9)$$

which is independent of the specific form of the distribution $g(\tau)$. It should be highlighted that the exact analytic results in Eqs. (8) and (9) for the infinite system ($N \to \infty$) are of practical interest, since they serve as a fairly accurate description for the emergence of AD in the finite system with large N. To validate the above argument, Fig. 1 plots the distribution of $\lambda_1, \ldots, \lambda_N$ with the parameters $N = 30$, $K = 5$, $w = 10$, and $\sigma = 0.4$ with a uniform distribution. The black squares denote the results numerically computed from Eq. (4). All the eigenvalues have strictly negative real parts, which implies that the coupled system (1) undergoes AD for the above choice of parameters. Interestingly, the structure of the characteristic eigenvalues in Eq. (4) is found to be well predicted by the continuous spectrum (the red solid line) and the discrete one (the red open circle) obtained from Eqs. (8) and (9), respectively.

The stability of AD is decided by whether all the characteristic roots λ in Eq. (4) have negative real parts $\mathrm{Re}(\lambda) < 0$. From the continuous spectrum in Eq. (9), we can easily get that AD is possible only if $K > 1+\sigma$. Consequently, one boundary for the stable AD regime is

$$K = 1 + \sigma, \quad (10)$$

which is independent of the distribution density $g(\tau)$. The other critical curve for the stable AD region is determined by the discrete spectrum as

$$\mathrm{Re}(\lambda_{\mathrm{DS}}) = 0, \quad (11)$$

where λ_{DS} is implicitly given in Eq. (6) depending on the specific distribution of τ_j. For $g(\tau)$ being a uniform distribution, the discrete spectrum is explicitly in Eq. (8). In Figs. 2(a) and 2(b), we plot the stable AD regions of the coupled system (1) with $N = 30$ oscillators in the parameter space of (σ, K) for two typical values of $w = 10$ and 5, where the time scales τ_j are uniformly distributed over $[1-\sigma, 1+\sigma]$. For both values of w, AD is stabilized within a pronounced interval of coupling strength for sufficiently large values of σ. The coupling interval of stable AD expands monotonically as σ increases gradually. The coupled system undergoes AD within a larger interval of coupling strength for a larger value of σ, which signals that the high level of diversity in time scales facilitates a stabilization of AD. In both subplots, the black squares mark the boundaries of the stable AD regions, which are obtained from direct numerical integrations of the coupled system (1) with random initial conditions. Clearly, it can be seen that the black squares lie almost exactly on the two solid lines defined by Eqs. (10) and (11), respectively. The above observation consolidates the fact that the stability of AD in the infinite system with time-scale diversity provides a fairly accurate description of AD in the large finite case.

From Figs. 2(a) and 2(b), one can also infer that the AD region strongly shrinks if the value of w decreases from 10 to 5, which indicates that the parameter w plays an important role for the time-scale diversity induced AD. Now we will explore the impact of w on AD. Figure 3(a) depicts the spread of the stable AD interval as a function of w for $\sigma = 0.4$. The coupling interval for stable AD strictly decreases as w decreases, and it vanishes at a critical threshold of $w_{\min} = 4.95$.

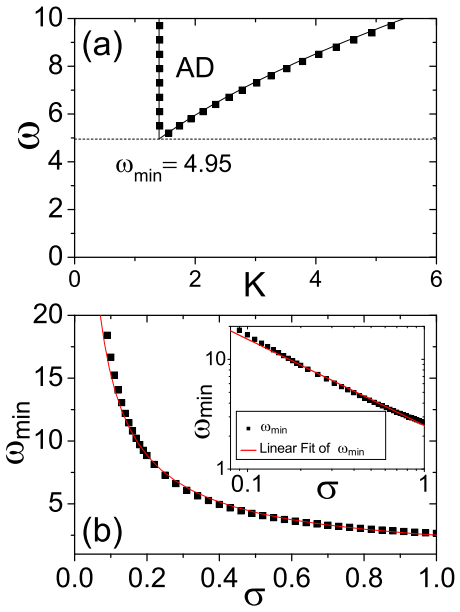

FIG. 3. (a) Stability region for AD of the coupled system (1) with $N = 30$ in the parameter space of (K, w) for a uniform distribution of $g(\tau)$ with $\sigma = 0.4$. The coupling interval for AD decreases monotonically as w decreases, and completely disappears if $w < w_{\min} = 4.95$. The black squares and the black solid line, respectively, denote the numerical simulations and the theoretical predictions as in Fig. 2. (b) The dependence of $w_{\min}$ on σ. The black square points of $w_{\min}$ are obtained as in (a). The red solid line is a power-law fit $w_{\min} \propto \sigma^{\gamma}$ with $\gamma = -0.76$, which is clearly demonstrated in the upper-right inset with the log-log plot.

Again, the numerical results denoted by the black squares agree well with the theoretical predictions plotted by the two black lines from Eqs. (10) and (11).

Figure 3(b) further depicts the dependence of $w_{\min}$ on σ. The behavior of $w_{\min}$ is well fitted by a power-law scaling

$$w_{\min} \propto \sigma^{\gamma} \tag{12}$$

with $\gamma = -0.76$ (the red solid line); this is clearly identified from the log-log plot in the upper-right inset of Fig. 3(b). $w_{\min}$ grows sharply as σ approaches zero, indicating that AD is difficult to achieve in the coupled system (1) if time scales are dispersed within a very narrow distribution. The value of $w_{\min}$ decreases monotonically as σ increases, and it saturates at around 2.65. Hence, AD is impossible in the coupled system (1) for any combinations of K and σ if $w < 2.65$.

From Fig. 3, one can infer that the intrinsic frequency w is critical to the phenomenon of AD induced by time-scale diversity. A low value of w tends to impede the occurrence of AD, and AD is totally eliminated once w is below a certain cutoff threshold. The underlying mechanism can be interpreted as the following physical intuition. For the coupled system to experience AD, one key ingredient is that the distribution of time scales is requested to be sufficiently disparate. In fact, the effective time scale of the individual jth Stuart-Landau oscillator is determined by $w\tau_j$. It is easy to obtain that the difference between the maximum and the minimum of the effective time scales $w\tau_j$ is $2w\sigma$. Clearly, w is involved to affect the variance of the distribution of effective time scales.

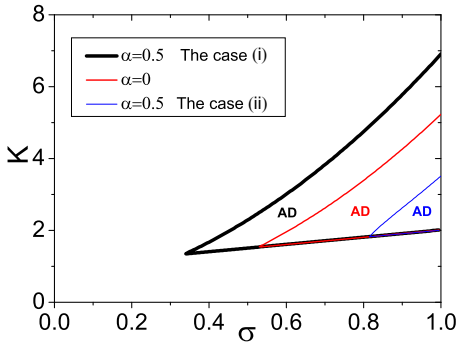

FIG. 4. Effect of the distribution of w_j on AD induced by time-scale diversity in the coupled system (1). The stability regions for AD are depicted in the parameter space of (σ, K) with w_j and τ_j independently and uniformly distributed over $[1-\sigma, 1+\sigma]$ and $[w-\alpha, w+\alpha]$, respectively. $N = 100$ and $w = 5$ are fixed. For $\alpha > 0$, a lot of different combinations for τ_j and w_j are possible, where the two extreme cases are (i) $\tau_j = 1+\sigma(2j-N-1)/(N-1)$ and $w_j = w+\alpha(2j-N-1)/(N-1)$, and (ii) $\tau_j = 1+\sigma(2j-N-1)/(N-1)$ and $w_{(N-j+1)} = w+\alpha(2j-N-1)/(N-1)$. The AD region expands for $\alpha = 0.5$ with the case (i) (enclosed by the black lines) and shrinks for $\alpha = 0.5$ with the case (ii) (enclosed by the blue lines) compared with that for $\alpha = 0$ (enclosed by the red lines), as the level of diversity for the effective time scales is enhanced in the case (i) and is weakened in the case (ii) by the distribution of w_j.

Decreasing w results in values of $w\tau_j$ distributed within a narrow interval. A lower value of w weakens the level of diversity of the effective time scales, which thus leads to less AD in the coupled system.

If the intrinsic frequencies w_j of the oscillators are further distributed within an interval according to a certain density, the AD region in the parameter space of (σ, K) can be either enlarged or shrunk depending on whether the level of diversity of the effective time scales $w_j\tau_j$ is enhanced or weakened. To validate this, we assume that both τ_j and w_j are uniformly distributed over $[1-\sigma, 1+\sigma]$ and $[w-\alpha, w+\alpha]$, respectively. As the two distributions of τ_j and w_j are independent, there are different combinations for $w_j\tau_j$ for the fixed values of σ and α, which yields different levels of diversity for the effective time scales $w_j\tau_j$. Here, to exclusively show the dual roles of the distribution of w_j on the occurrence of AD, we consider two extreme combinations of τ_j and w_j as (i) $\tau_j = 1+\sigma(2j-N-1)/(N-1)$ and $w_j = w+\alpha(2j-N-1)/(N-1)$, and (ii) $\tau_j = 1+\sigma(2j-N-1)/(N-1)$ and $w_{(N-j+1)} = w+\alpha(2j-N-1)/(N-1)$. The differences between the largest and smallest values of $w_j\tau_j$ for the cases (i) and (ii) are $2(w\sigma+\alpha)$ and $2(w\sigma-\alpha)$, which reflect the levels of diversity for the two combinations of $w_j\tau_j$. In the presence of the distribution of w_j, i.e., $\alpha > 0$, the level of diversity of the effective time scales is strengthened for the case (i) and reduced for the case (ii). Thus, AD will be more preferable for the case (i) and be less possible for the case (ii), compared with that for the identical frequencies $w_j = w$ with $\alpha = 0$. Figure 4 plots the AD regions in the parameter space of (σ, K) for $\alpha = 0$ and $\alpha = 0.5$ with the two cases (i) and (ii) for w_j and τ_j. $N = 100$ and $w = 5$ are fixed. We indeed observe that AD occurs for a larger set of parameters for the case (i) (bounded by the black lines) and a smaller one

for the case (ii) (bounded by the blue lines) when compared with that for $\alpha = 0$ (bounded by the red lines). Note that the lower critical coupling strength for the onset of AD for all three cases is well predicted by Eq. (10).

B. Coupled nonlinear oscillators of a general form

More importantly, our theory of predicting AD is not restricted to the limit-cycle model of a Stuart-Landau oscillator, which holds fairly generally for many other oscillator models with periodic or even chaotic behaviors. Consider a general form of globally and diffusively coupled oscillators with time-scale diversity

$$\dot{X}_j = \tau_j F(X_j) + \frac{K}{N}\sum_{k=1}^{N}(X_k - X_j), \tag{13}$$

where $X_j \in R^n$ $(j = 1, \ldots, N)$ is the n-dimensional state vector of the jth element, and τ_j $(j = 1, \ldots, N)$ is the same as that used in Eq. (1). The single uncoupled dynamical system $\dot{X}_j = F(X_j)$ exhibits oscillatory (periodic or chaotic) dynamics accompanied by an unstable focus X^*. Without loss of generality, we assume that the focus X^* is unstable due to a pair of conjugate characteristic eigenvalues $\alpha \pm i\beta$ $(\alpha > 0, \beta \neq 0)$, and all its other associated characteristic eigenvalues have negative real parts.

The occurrence of AD in the coupled systems (13) means that the fixed-point solution $X_1 = X_2 = \cdots = X_N = X^*$ is stabilized. The requirements of stabilizing AD can be identified by performing a standard linear stability analysis of the death solution of Eq. (13). Following a similar approach to that in the previous case for globally coupled Stuart-Landau oscillators (1), the discrete and continuous spectra responsible for the boundaries of the stable AD region are now given by

$$\frac{1}{K} = \int_{1-\sigma}^{1+\sigma} \frac{g(\tau)d\tau}{\lambda + K - \tau(\alpha + i\beta)} \tag{14}$$

and

$$\lambda_{\mathrm{CS}} = \tau(\alpha + i\beta) - K, \text{ where } 1 - \sigma \leqslant \tau \leqslant 1 + \sigma, \tag{15}$$

respectively. Again for a uniform distribution $g(\tau)$ as in Eq. (7), the discrete spectrum is further explicitly expressed as

$$\lambda_{\mathrm{DS}} = \frac{2\sigma(\alpha + i\beta)}{\exp\left[\frac{2\sigma(\alpha+i\beta)}{K}\right] - 1} - K + (1 + \sigma)(\alpha + i\beta). \tag{16}$$

By dividing α $(\alpha > 0)$ from both sides of Eqs. (15) and (16), one can find that the two equations are reduced to the same forms of Eqs. (8) and (9), where w is replaced by β/α and K is rescaled to K/α (λ_{DS} and λ_{CS} are also rescaled to $\lambda_{\mathrm{DS}}/\alpha$ and $\lambda_{\mathrm{CS}}/\alpha$). From a thorough analysis of AD in coupled Stuart-Landau oscillators, one can directly deduce that once $\beta/\alpha > 2.56$ is fulfilled, AD can be stabilized in the coupled system (13) for suitable values of K and σ.

For illustration and verification, in the following we will present a study with the chaotic Rössler oscillator: $\dot{x} = -y - z$, $\dot{y} = x + ay$, $\dot{z} = b + z(x - c)$. The parameters $a = 0.15$, $b = 0.2$, and $c = 10.0$ are used. The single Rössler oscillator has a chaotic phase-coherent attractor, accompanied by an unstable focus $X^* = (x^*, y^*, z^*)^T$ near the origin. This focus is given as $X^* = (x^*, y^*, z^*)^T$ with $x^* = -ay^*$, $y^* = -z^*$, and $z^* = \frac{c - \sqrt{c^2 - 4ab}}{2a}$, whose associated characteristic eigenvalues are $0.0740 + 0.9972i$, $0.0740 - 0.9972i$, and -9.9950. $\alpha = 0.0740$ and $\beta = 0.9972$ are fixed and will be used in Eqs. (15) and (16), respectively. Here $\beta/\alpha = 13.48 > 2.56$ is satisfied, thus AD is possible. Figure 5(a) shows the bifurcation diagram of $N = 100$ coupled chaotic Rössler oscillators with $\sigma = 0.4$, which plots the local maxima of the mean field $X = \frac{1}{N}\sum_{k=1}^{N} x_j$ as a function of the coupling strength K. With increasing K, AD is found to be stabilized for $0.1 < K < 0.72$. Figure 5(b) further depicts the stable AD region in the parameter space of (σ, K). The black squares marking the boundary of the stable AD region are obtained by direct numerical simulations as in Fig. 5(a). All the black squares are almost exactly located on the lower and upper critical lines decided by the continuous and discrete spectra in Eqs. (15) and (16), which clearly corroborates the validity of the theory in coupled chaotic Rössler oscillators with time-scale diversity.

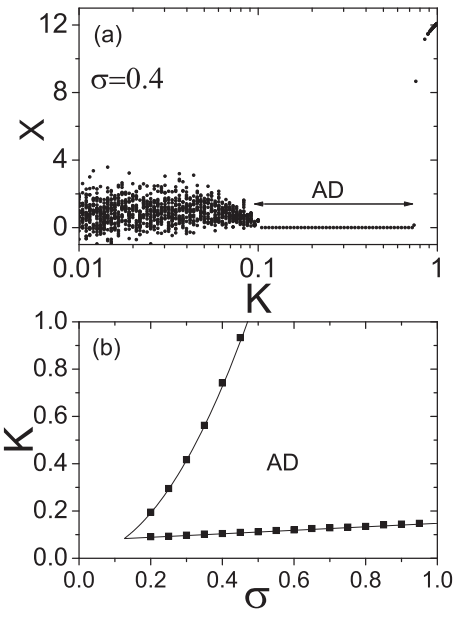

FIG. 5. (a) Bifurcation diagram by plotting the local maxima of the mean of the x_j $(j = 1, \ldots, N)$ for the globally coupled chaotic Rössler oscillators with $N = 100$ and a uniform distribution of $g(\tau)$ with $\sigma = 0.4$. With increasing the value of K, AD is stabilized within a certain coupling interval of $0.1 < K < 0.72$. (b) Stability region for AD in the parameter space of (σ, K). The black squares are numerical results for the AD boundary from direct integrations of the $N = 100$ coupled chaotic Rössler oscillators as in (a), where the lower and upper solid lines are the theoretical predictions from Eqs. (15) and (16) with the chaotic Rössler oscillator model.

III. DISCUSSIONS

In this section, we would like to present the following discussions about our theory and results:

(i) As mentioned in the Introduction, Monte *et al.* have addressed the emergence of AD in globally coupled oscillators with time-scale diversity [40], where they developed a novel technique of *order-parameter expansion* to predict the onset of AD. With their method, one can derive that, for

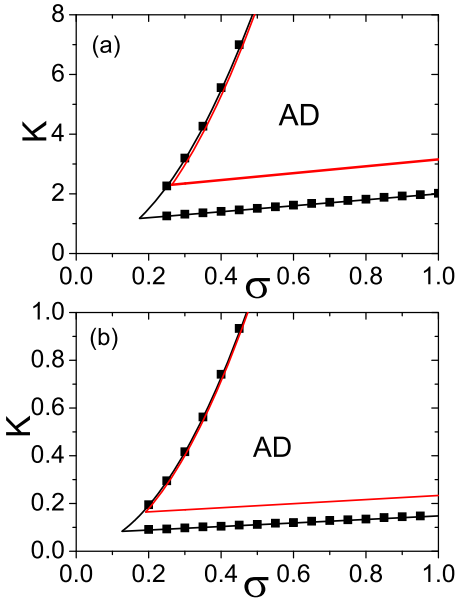

FIG. 6. Comparison of the bifurcation boundaries of the AD region by the method of order-parameter expansion in [40] with our results for (a) coupled Stuart-Landau oscillators and (b) coupled chaotic Rössler oscillators. The time scales τ_j are uniformly distributed over $[1-\sigma, 1+\sigma]$. The prediction of AD from the method of order-parameter expansion in [40] is indicated by the red solid lines. Our theoretical prediction is marked by the black solid lines, and the black squares denote the numerical observation of AD, which are the same as in Figs. 2(a) and 5(b), respectively. Our theory gives rise to a better prediction of the boundaries of the AD region compared with the method of order-parameter reduction.

τ_j uniformly distributed over $[1-\sigma, 1+\sigma]$, the asymptotic behavior for the lower and upper boundaries of the AD region in the parameter space of (σ, K) is given by

$$K = 2\alpha(1+\sigma/\sqrt{3}) \tag{17}$$

and

$$K = \alpha(\beta^2/\alpha^2 - 1)\sigma^2/3, \tag{18}$$

respectively, where α and β are the real and imaginary parts of the uncoupled system's unstable characteristic eigenvalue ($a = 1$ and $\beta = w$ for Stuart-Landau oscillator). Figures 6(a) and 6(b) plot the predictions of Eqs. (17) and (18) by the red solid lines in the parameter space of (σ, K) for coupled Stuart-Landau oscillators and coupled chaotic Rössler oscillators, respectively, where all the other results are correspondingly reproduced from Figs. 2(a) and 5(b). It is found that the lower (upper) critical coupling strength K for AD is larger (smaller) than our results obtained from the direct numerical simulations of the full coupled systems. Our theory leads to a better prediction of both the lower and the upper critical coupling strength K for AD. This is because the stability of AD in our theory is identified by analyzing the eigenvalues of the full coupled system, whereas the onset of AD with the method of *order-parameter expansion* by Monte *et al.* is estimated from a reduced system [40]. Our method is elementary and rigorous, thus it leads to a better reconciliation of theoretical prediction and numerical observations.

(ii) As pointed out in Sec. II, the continuous spectrum is independent of the time-scale distribution $g(\tau)$, while the discrete spectrum depends on the specific form of the distribution $g(\tau)$. In this study, our main attention is focused on the case of τ_j being pulled from a uniform distribution. The reason is that, for a uniform distribution $g(\tau)$, the discrete spectrum can be derived analytically [Eq. (8) or Eq. (16)]. In general, for other types of nonuniform distribution $g(\tau)$, the discrete spectrum is implicitly given in Eq. (6) or Eq. (14), whose analytical expression cannot be obtained explicitly. However, the root of λ in Eq. (6) or Eq. (14) can be solved numerically. In fact, for other nonuniform distributions, we got quite similar results as in Fig. 2 for coupled Stuart-Landau oscillators and Fig. 5 for coupled chaotic Rössler oscillators.

(iii) Time-scale diversity is certainly one important way in which coupled oscillators may be nonidentical. However, it is not fully general to characterize the heterogeneity of interacting systems. For example, in Eq. (13) one can see that the τ_j values essentially play the role of a rescaling of time. But while these τ_j values vary among oscillators, the intrinsic dynamics term $F(X_j)$ still remains identical for all oscillators, and thus the homogeneous fixed point $X_1 = X_2 = \cdots = X_N = X^*$ is always an AD solution of the coupled system (13) independent of the distribution of τ_j. In terms of modeling the role of disorder in systems of coupled oscillators, the time-scale diversity captures one aspect. With the introduction of a more general form of disorder for the parameters of individual oscillators, such that the intrinsic dynamics $F(X_j)$ is nonidentical, the solution of AD manifested through a homogeneous steady state is usually destroyed or even no longer exists. Our method, therefore, is not applicable anymore. It is a promising direction for future study to develop other innovative frameworks with new technology to explore the collective dynamics of a globally coupled system in the presence of diversity in both the time scales and the intrinsic parameters of individual elements.

IV. CONCLUSION

In conclusion, via a rigorous linear stability analysis, we have addressed the emergence of AD in ensembles of globally coupled oscillators with time-scale diversity. We have carried out a thorough study of AD in a paradigmatic system of globally coupled Stuart-Landau limit-cycle oscillators with uniformly distributed time scales. We have found that the structure of the characteristic eigenvalues of a large finite system is nicely characterized by the continuous and discrete spectra of the system in its thermodynamic limit. The onset of AD thus can be well predicted theoretically from the analysis of the continuous and discrete spectra. We have confirmed the argument by observing that the AD boundaries from direct numerical simulations are in good agreement with the critical curves from the continuous and discrete spectra. The intrinsic frequency w has been reported to play a crucial role for the time-scale diversity induced AD in coupled Stuart-Landau oscillators. It is revealed that the lower the intrinsic frequency w, the smaller is the set of parameters for stable AD. If the value of w is below a certain threshold, AD is impossible for any coupling strength and any level of diversity in time scales. Finally, we have extended the study to a general dynamical

system of globally coupled oscillators with dispersed time scales, where a nice prediction for the occurrence of AD in coupled chaotic Rössler oscillators has been verified. In our simulations, we have used many other parameter values for the Rössler oscillator, and we also tested several other chaotic oscillator models. For each case, a quite good prediction for the onset of AD as in Fig. 5 has been obtained. As many functional processes of real-world systems take place with different time scales, we expect that our results are relevant for various applications, such as in biology, ecology, and neuroscience.

ACKNOWLEDGMENTS

We are grateful to the two anonymous reviewers for their very constructive comments, which helped to greatly improve this paper. W.Z. was supported by Research Starting grants from South China Normal University (8S0340) and a project supported by Guangdong Province Universities and Colleges Pearl River Scholar Funded Scheme (2018). M.Z. was supported by the National Natural Science Foundation of China under Grant No. 11475253. J.K. was supported by the Russian Science Foundation (Grant No. 17-15-01263).

[1] Y. Kuramoto, *Chemical Oscillations, Waves, and Turbulence* (Springer, Berlin, 1984).
[2] A. Pikovsky, M. Rosenblum, and J. Kurths, *Synchronization: A Universal Concept in Nonlinear Sciences* (Cambridge University Press, Cambridge, 2001).
[3] J. D. Murray, *Mathematical Biology*, 2nd ed. (Springer, Berlin, 1993).
[4] G. Saxena, A. Prasad, and R. Ramaswamy, Phys. Rep. **521**, 205 (2012).
[5] A. Koseska, E. Volkov, and J. Kurths, Phys. Rep. **531**, 173 (2013).
[6] A. Prasad, Y. C. Lai, A. Gavrielides, and V. Kovanis, Phys. Lett. A **318**, 71 (2003).
[7] T. Biwa, S. Tozuka, and T. Yazaki, Phys. Rev. Appl. **3**, 034006 (2015).
[8] N. Thomas, S. Mondal, S. A. Pawar, and R. I. Sujith, Chaos **28**, 033119 (2018).
[9] Y. Yamaguchi and H. Shimizu, Physica D **11**, 212 (1984).
[10] K. Bar-Eli, Physica D **14**, 242 (1985).
[11] D. V. Ramana Reddy, A. Sen, and G. L. Johnston, Phys. Rev. Lett. **80**, 5109 (1998).
[12] D. V. Ramana Reddy, A. Sen, and G. L. Johnston, Physica D **129**, 15 (1999).
[13] F. M. Atay, Phys. Rev. Lett. **91**, 094101 (2003).
[14] W. Zou and M. Zhan, Phys. Rev. E **80**, 065204(R) (2009).
[15] C. G. Yao, W. Zou, and Q. Zhao, Chaos **22**, 023149 (2012).
[16] S. R. Huddy and J. Sun, Phys. Rev. E **93**, 052209 (2016).
[17] K. Konishi, Phys. Rev. E **68**, 067202 (2003).
[18] K. Konishi, Int. J. Bifurcation Chaos **17**, 2781 (2007).
[19] K. Konishi and N. Hara, Phys. Rev. E **83**, 036204 (2011).
[20] R. Karnatak, R. Ramaswamy, and A. Prasad, Phys. Rev. E **76**, 035201(R) (2007).
[21] X. M. Zhang, Y. C. Wu, and J. H. Peng, Int. J. Bifurcation Chaos **21**, 225 (2011).
[22] N. N. Zhao, Z. K. Sun, X. L. Yang, and W. Xu, Phys. Rev. E **97**, 062203 (2018).
[23] V. Resmi, G. Ambika, and R. E. Amritkar, Phys. Rev. E **84**, 046212 (2011).
[24] A. Sharma, P. R. Sharma, and M. D. Shrimali, Phys. Lett. A **376**, 1562 (2012).
[25] N. K. Kamal, P. R. Sharma, and M. D. Shrimali, Phys. Rev. E **92**, 022928 (2015).
[26] A. Sharma and M. D. Shrimali, Phys. Rev. E **85**, 057204 (2012).
[27] T. Banerjee and D. Ghosh, Phys. Rev. E **89**, 052912 (2014).
[28] T. Banerjee and D. Ghosh, Phys. Rev. E **89**, 062902 (2014).
[29] T. Banerjee, D. Biswas, D. Ghosh, B. Bandyopadhyay, and J. Kurths, Phys. Rev. E **97**, 042218 (2018).
[30] D. G. Aronson, G. B. Ermentrout, and N. Kopell, Physica D **41**, 403 (1990).
[31] G. B. Ermentrout, Physica D **41**, 219 (1990).
[32] R. E. Mirollo and S. H. Strogatz, J. Stat. Phys. **60**, 245 (1990).
[33] L. Rubchinsky and M. Sushchik, Phys. Rev. E **62**, 6440 (2000).
[34] J. Yang, Phys. Rev. E **76**, 016204 (2007).
[35] Y. Wu, W. Q. Liu, J. H. Xiao, W. Zou, and J. Kurths, Phys. Rev. E **85**, 056211 (2012).
[36] J.-W. Ryu, J.-H. Kim, W.-S. Son, and D.-U. Hwang, Chaos **27**, 083119 (2017).
[37] Z. Hou and H. Xin, Phys. Rev. E **68**, 055103(R) (2003).
[38] W. Liu, X. Wang, S. Guan, and C. H. Lai, New J. Phys. **11**, 093016 (2009).
[39] C. S. Shen, H. S. Chen, and Z. H. Hou, Chaos **24**, 043125 (2014).
[40] S. De Monte, F. D'Ovidio, and E. Mosekilde, Phys. Rev. Lett. **90**, 054102 (2003).
[41] S. De Monte and F. D'Ovidio, Europhys. Lett. **58**, 21 (2002).